Electronic Supporting Information

ESIPT-capable 2,6-di(1H-imidazol-2-yl)phenols with very strong fluorescent sensing signals towards Cr(III), Zn(II) and Cd(II): molecular variation effects on turn-on efficiency

Abiodun O. Eseola,[§,‡,*] Masroor Bangesh,[†] Helmar Görls,[‡] Winfried Plass,[‡,*]

[§]Materials Chemistry group, Department of Chemical Sciences, Redeemer's University Ede, Osun State, Nigeria.

[‡]Institut für Anorganische und Analytische Chemie, Friedrich-Schiller-Universität Jena, Humboldtstr. 8, D-07743 Jena, Germany.

[†]Department of Chemistry, Hazara University, Mansehra (Khyber Pakhtunkhwa) Pakistan.

---

[*] Corresponding authors: Dr. A. O. Eseola: Materials Chemistry group, Department of Chemical Sciences, Redeemer's University Ede, Osun State, Nigeria; Tel.: +49(0)15218016407, +493641948138. e-mail: bioduneseola@hotmail.com; biodun.eseola@uni-jena.de; Prof. Dr. W. Plass; Address – Institut für Anorganische und Analytische Chemie, Friedrich-Schiller-Universität Jena, Humboldtstr. 8, D-07743 Jena, Germany; Tel.: +49 3641 948130; Fax: +49 3641948132; e-mail: sekr.plass@uni-jena.de

Table S1: Crystal data and refinement details for the X-ray structure determinations of the compounds **1**-CoOAc, **2**-$CdClO_4$, **2**-$HClO_4$ and **2**-$Zn(ClO_4)_2$.

Compound	**1**-CoOAc	**2**-$CdClO_4$	**2**-$HClO_4$	**2**-$Zn(ClO_4)_2$
formula	$C_{81.5}H_{69.5}Co_2N8O_{9.5}$	$C_{123}H_{105}Cd_2ClN_{12}O_{19}$	$C_{84}H_{78}Cl_2N_8O_{20}$	$C_{123}H_{107}Cl_3N_{12}O_{27}Zn_2$
fw ($g\cdot mol^{-1}$)	1430.81	2315.44	1594.48	2422.30
T (°C)	-140(2)	-140(2)	-140(2)	-140(2)
crystal system	monoclinic	monoclinic	triclinic	monoclinic
space group	C 2/c	C 2/c	$P\,\bar{1}$	$P\,2_1/n$
a/ Å	33.3550(5)	38.0152(7)	9.9752(4)	17.1244(4)
b/ Å	26.9197(3)	20.0199(3)	20.4504(8)	21.5681(5)
c/ Å	22.0520(3)	38.3943(7)	20.9362(9)	33.1488(7)
α/°	90	90	113.980(2)	90
β/°	119.388(1)	117.063(1)	102.087(2)	91.886(1)
γ/°	90	90	95.194(2)	90
V/$Å^3$	17252.6(4)	26020.9(8)	3741.3(3)	12236.6(5)
Z	8	8	2	4
ρ ($g\cdot cm^{-3}$)	1.102	1.182	1.412	1.315
μ (cm^{-1})	4.39	4.11	1.7	5.34
measured data	48340	92971	40529	69233
data with $I > 2\sigma(I)$	11025	14514	6849	15472
unique data (R_{int})	14581/0.0653	28370/0.1190	16167/0.1535	27256/0.1406
wR_2 (all data, on F^2)[a]	0.2993	0.3675	0.3473	0.2572
R_1 ($I > 2\sigma(I)$)[a]	0.1009	0.1311	0.1769	0.1187
S[b]	1.042	1.097	1.091	1.054
Res. dens./$e\cdot Å^{-3}$	2.321/-0.784	1.907/-1.049	1.611/-1.366	1.304/-1.174
absorpt method	multi-scan	multi-scan	multi-scan	multi-scan
absorpt corr $T_{min/max}$	0.5879/0.7456	0.6351/0.7456	0.6295/0.7456	0.6681/0.7456
CCDC No.	motif	motif	motif	motif

[a] Definition of the R indices: $R_1 = (\Sigma||F_o|-|F_c||)/\Sigma|F_o|$; $wR_2 = \{\Sigma[w(F_o^2-F_c^2)^2]/\Sigma[w(F_o^2)^2]\}^{1/2}$ with $w^{-1} = \sigma^2(F_o^2) + (aP)^2+bP$; $P = [2F_c^2 + Max(F_o^2]/3$; [b] $s = \{\Sigma[w(F_o^2-F_c^2)^2]/(N_o-N_p)\}^{1/2}$.

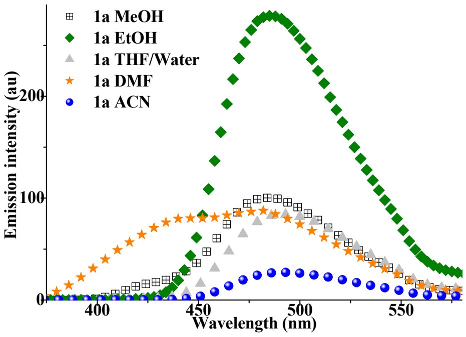

Fig. S1: Emission spectra of **1a** in various solvents showing that **1a** possess the lowest emission intensity in acetonitrile solution

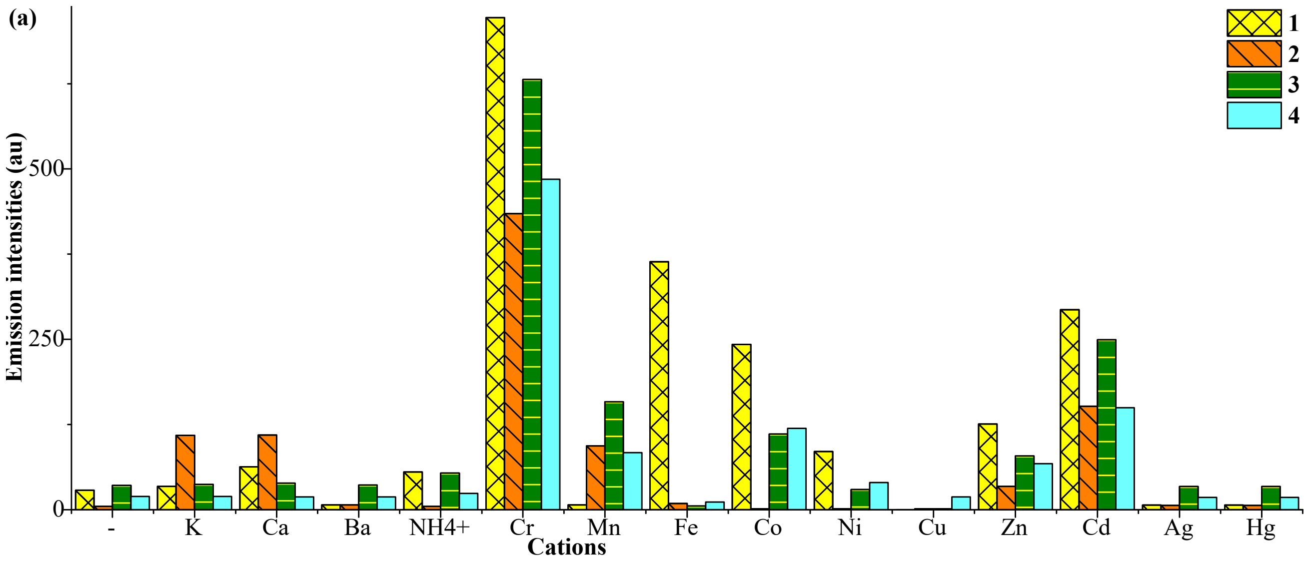
(a)
Emission intensities (au)
0
250
500
-
K
Ca
Ba
NH4+
Cr
Mn
Fe
Co
Ni
Cu
Zn
Cd
Ag
Hg
Cations
1
2
3
4

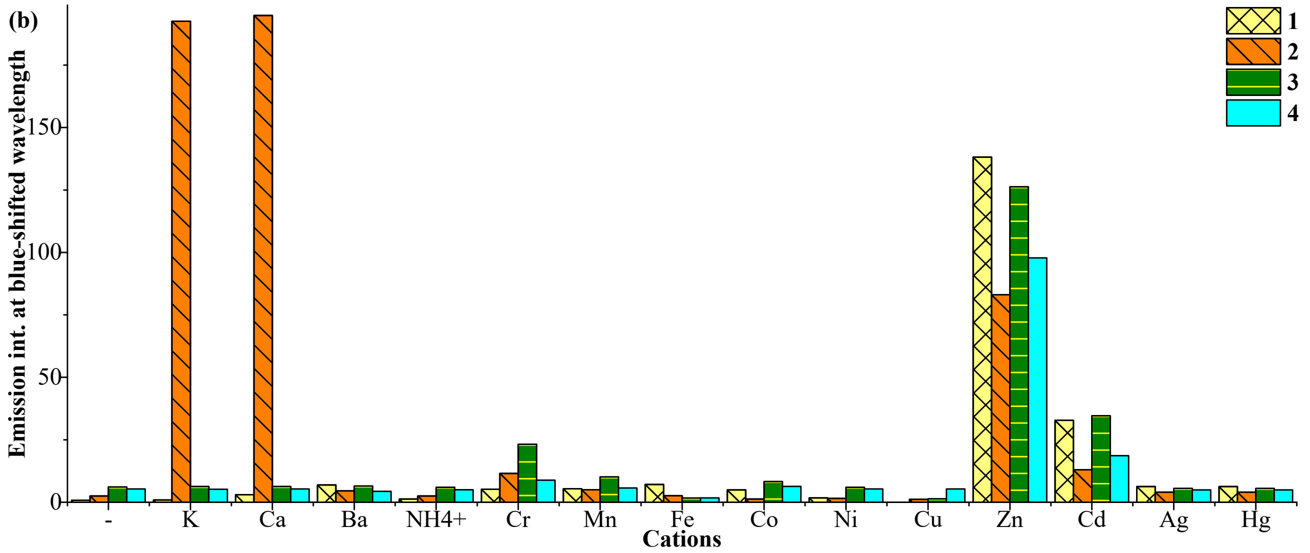
(b)
Emission int. at blue-shifted wavelength
0
50
100
150
-
K
Ca
Ba
NH4+
Cr
Mn
Fe
Co
Ni
Cu
Zn
Cd
Ag
Hg
Cations
1
2
3
4

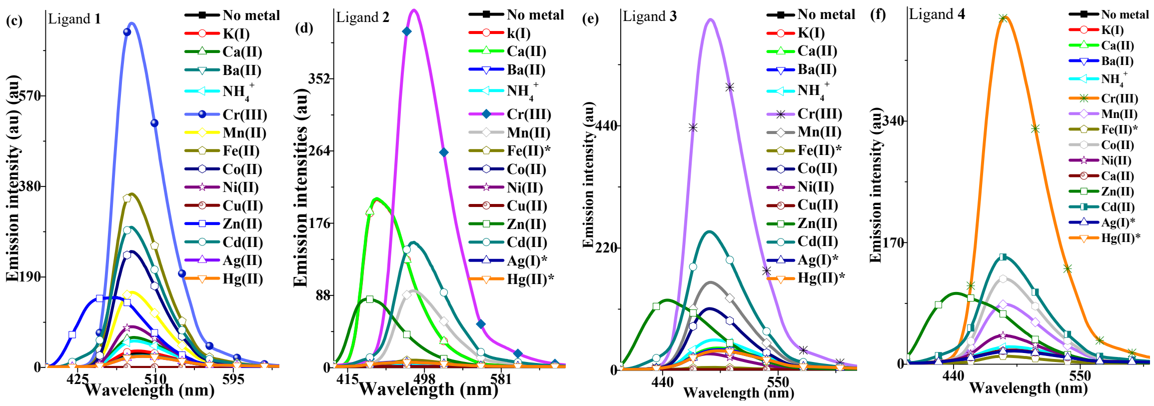
(c)
Ligand 1
Emission intensity (au) (au)
0
190
380
570
425
510
595
Wavelength (nm)
No metal
K(I)
Ca(II)
Ba(II)
NH_4^+
Cr(III)
Mn(II)
Fe(II)
Co(II)
Ni(II)
Cu(II)
Zn(II)
Cd(II)
Ag(II)
Hg(II)
(d)
Ligand 2
Emission intensities (au)
0
88
176
264
352
415
498
581
Wavelength (nm)
No metal
k(I)
Ca(II)
Ba(II)
NH_4^+
Cr(III)
Mn(II)
Fe(II)*
Co(II)
Ni(II)
Cu(II)
Zn(II)
Cd(II)
Ag(I)*
Hg(II)*
(e)
Ligand 3
Emission intensity (au)
0
220
440
440
550
Wavelength (nm)
No metal
K(I)
Ca(II)
Ba(II)
NH_4^+
Cr(III)
Mn(II)
Fe(II)*
Co(II)
Ni(II)
Cu(II)
Zn(II)
Cd(II)
Ag(I)*
Hg(II)*
(f)
Ligand 4
Emission intensity (au)
0
170
340
440
550
Wavelength (nm)
No metal
K(I)
Ca(II)
Ba(II)
NH_4^+
Cr(III)
Mn(II)
Fe(II)*
Co(II)
Ni(II)
Ca(II)
Zn(II)
Cd(II)
Ag(I)*
Hg(II)*

Fig. S2: Bar chart presentation of emission intensities for probes **1** – **4** showing (a) comparison for Cr^{3+} turn-on at ligand emission wavelength and (b) comparison for Zn^{2+} at its blue-shifted wavelength. (c) – (f) show emissions on addition of various cations to probes **1** – **4** respectively.

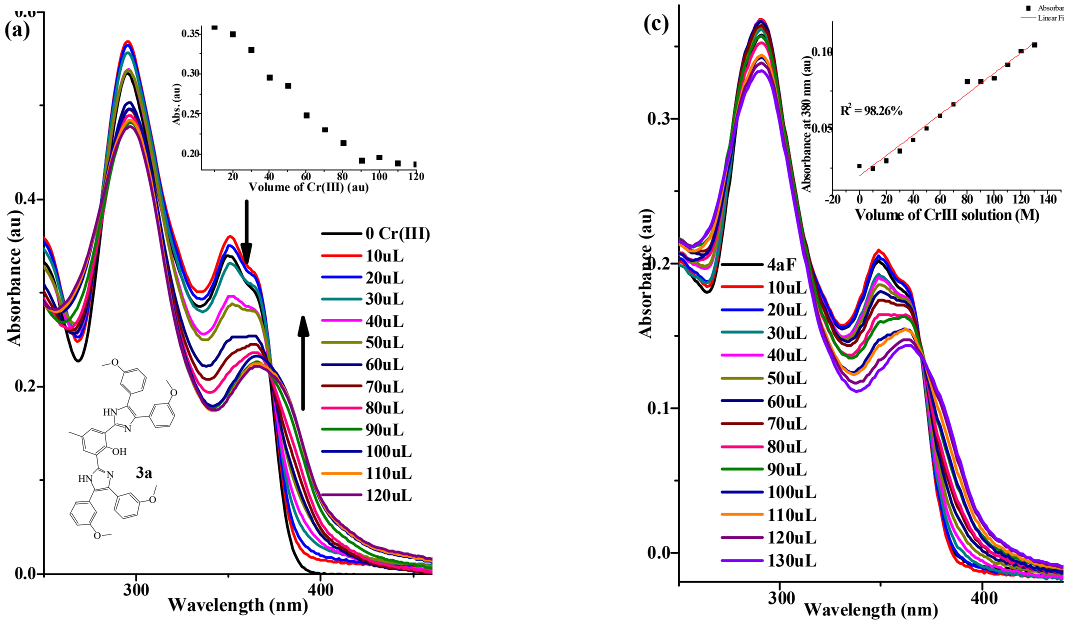

Fig. S3: Stacked absorption spectra for Cr^{3+} titration against **(a) 3** and **(b) 4** respectively.

S4: Quantum mechanical calculations (further details)

Model Structures

The model structure 1L is 2-imidazolyl-phenol, a moiety with intramolecular hydrogen bond, and car- rying entire bidentate coordination capability of ligands as determined in crystal structure of 7-$CoCl_2$ complex (Fig 2 *main manuscript*). Model structure 2L is planar 2,6-di(imidazolyl)phenol, an unsubstituted analogue of synthesised ligands **1** and its variously substituted derivatives shown in Scheme 1 (*main manuscript*). Structure 2LR is a different conformation of 2L with one imidazole ring rotated by 90° out of plane of rest of molecule.

Chromium(III) is known to exist as hexacarbonyl and hexaaqua complex cations in octahedral geome- tries, therefore 1L chelates through phenolic oxygen and imidazole nitrogen to Cr^{3+} while replacing two water molecules in coordination shell of chromium (III) hexaaqua cation, as depicted in structure 1L-Cr^{3+}. This structure is chosen to capture the essential features of Cr^{3+} coordination with ligands 1– 6.

Orbital Active Spaces

Active spaces of orbitals used to optimise multi-configuration self consistent field (MCSCF) wave func- tions were chosen to maximally include electrons contributing towards static correlation due to multiref- erence nature of electronic states.

1L Active Spaces: In case of 1L, the smallest active space is composed of all conjugated π electrons (in a^{II} symmetry orbitals) of imidazole and phenoxy rings denoted as CAS(10, 10) which means 10 active electrons in 10 orbitals of the $\pi-$conjugated skeleton of atoms

2 – 9, and atoms 10 – 11 in Fig. 2 Inclusion of lone electron pair of nitrogen atom 12 into orbital active space gives rise to CAS(12,11) while further including two electrons in oxygen *p* orbital perpendicular to C*s* plane of 1L results into CAS(14, 12). These active spaces describe $\pi\pi^*$ transitions, whereas inclusion of *n* orbitals (a^{I} symme- try) of phenolic oxygen or imidazolic nitrogen 12 did not affect low lying A^{I} electronic states, and A^{II} accessed through $n\pi^*$ transitions lie towards higher end of energy spectrum.

1L-Cr^{3+} Active Spaces: Calculations confirmed that low lying A^{I} states only involve π orbitals of imidazolyl phenol moiety with *d* orbitals of chromium. Hence optimisation of orbitals through MCSCF procedure retained two *d* orbitals of a^{II} symmetry and one of a^{I} symmetry in active spaces of A^{I} electronic states of our interest. Other electronic states involving interactions of *n* orbitals on 1L moiety with *d* electrons, or those involving interaction of water ligands with Cr lie towards higher energies. In this light, inclusion of unpaired chromium d^3 electrons (1L-Cr^{3+}) gives rise to CAS(13, 13), CAS(15, 14), and CAS(17, 15) in parallel to above mentioned 1L active spaces CAS(10, 10), CAS(12, 11), and CAS(14,12) respectively.

Actual calculations for 1L-Cr^{3+} are done with CAS(13, 13), CAS(15, 14), CAS(15, 13), and OR- MAS(17, 14) whereas last two active spaces result after omissions from active space, of a highest energy diffuse π orbital unoccupied in reference determinant. Occupation restricted multiple active space (OR- MAS) reference consisted of two sub-spaces of 10 occupied orbitals (containing 17 electrons) and 4 vir- tual orbitals, while multiple reference determinants were generated through full configuration interaction (CI) within each sub-space and exciting only single, double, triple, quadruple, quintuple, and sextuple (SDTQ56) electrons between two sub-spaces. First order MCSCF calculations are denoted CAS(*x, y*) or ORMAS(x, y) like above, and second order energy correction via multireference perturbation theory over same active size is denoted MRPT2(x, y).

Table S2: Energies (eV) and symmetries of active space orbitals shown in Fig S-2, and electronic con- figurations of few most dominant Slater determinants in each state weighted by square of CI coefficient (c^2). Onle a single representative spin congener of each given electronic configu- ration is shown.

	1L								1L-Cr^{3+}							
ψ	40	41	42	43	44	45	46		70	71	72	73	74	75	76	
	a"	a"	a"	a"	a"	a"	a"	c_i^2	a"	a"	a"	a’	a"	a"	a"	c_i^2
eV	-3.3	-1.6	0	6.9	10.3	11.5	12.9		-1.9	-1.7	-0.9	-0.8	0	6.6	9.9	
0A’	↿⇂	↿⇂	↿⇂					0.81	↿⇂	↿⇂	↿	↿	↿			0.46
	↿⇂		↿⇂		↿⇂			0.01	↿⇂	↿	↿	↿	↿⇂			0.24
	↿⇂	↿⇂		↿⇂				0.01	↿	↿⇂	↿⇂	↿	↿			0.07
									↿	↿	↿⇂	↿	↿⇂			0.04
									↿	↿⇂	↿	↿	↿⇂			0.01
1A’	↿⇂	↿	↿⇂	⇂				0.15	↿	↿⇂	↿	↿	↿	⇂		0.10
	↿⇂	↿⇂	⇂	↿				0.08	↿⇂	↿	↿	↿	↿		⇂	0.05
	↿⇂	↿⇂	⇂		↿			0.07	↿	↿	↿	↿	↿⇂	⇂		0.04
	⇂	↿⇂	↿⇂		↿			0.03	↿⇂	↿⇂	↿	↿			↿	0.03
	↿⇂	↿⇂	⇂			↿		0.01	↿⇂	↿⇂	↿	↿		↿		0.03
2A’	↿⇂	↿⇂	⇂	↿				0.18	↿⇂	↿	↿	↿	↿	⇂		0.21
	↿⇂	↿⇂		↿⇂				0.07	↿⇂	↿⇂	↿	↿		↿		0.10
	⇂	↿⇂	↿⇂	↿				0.05	↿⇂		↿	↿	↿⇂	↿		0.08
	↿⇂	⇂	↿⇂	↿				0.04	↿	↿	↿⇂	↿	↿	⇂		0.02
	↿⇂	↿⇂	⇂		↿			0.02	↿	↿	↿	↿	↿⇂	⇂		0.02
3A’	↿⇂	↿⇂		↿⇂				0.13	↿⇂	↿	↿	↿	↿	⇂		0.20
	⇂	↿⇂	↿⇂	↿				0.08	↿⇂	↿⇂	↿	↿		↿		0.10
	↿⇂	↿⇂	⇂	↿				0.07	↿⇂		↿	↿	↿⇂	↿		0.06
	↿⇂	↿⇂	⇂			↿		0.04	↿	↿⇂	↿	↿	↿		⇂	0.05
	↿⇂	↿⇂	⇂				↿	0.02	↿	↿	↿	↿	↿⇂		⇂	0.03

Table S3: Vertical excitation energies (eV) relative to ground state singlet $^{1}0\mathrm{A}^{\mathrm{I}}$ (1L) or ground state quartet $^{1}0\mathrm{A}^{\mathrm{I}}$ (1L-Cr^{3+}), corresponding wavelength in nm and oscillator strengths (f) in brackets. All MCSCF and MRPT2 calculations with 6-31+G* basis and TD-B3LYP calcula- tions with def2-TZVP basis. Orbitals optimised with state-averaged MCSCF, and subsequent state specific MRPT2 energies.

	1L eV/ nm/ ($f \times 10^2$)				1L-Cr^{3+} eV/ nm/ ($f \times 10^2$)		
	^{1}1A$'$	^{1}2A$'$	^{1}3A$'$		^{4}1A$'$	^{4}2A$'$	^{4}3A$'$
CAS(10,10)	4.50 275 (4.00)	5.99 207 (19.00)	6.72 185 (21.00)	CAS(13,13)	3.43 362 (0.02)	4.12 301 (0.02)	4.36 284 (3.74)
MRPT2(10,10)	4.12 301	5.08 244	5.64 220	MRPT2(13,13)	3.19 389	3.56 348	3.72 333
CAS(12,11)	4.51 275 (5.00)	5.95 208 (26.00)	6.73 184 (13.00)	CAS(15,13)	3.44 361 (0.02)	4.00 310 (0.05)	4.30 288 (4.36)
MRPT2(12,11)	4.12 301	4.90 253	5.86 212	MRPT2(15,13)	3.08 403	3.48 356	3.66 339
CAS(14,12)	4.47 277 (5.00)	5.93 209 (26.00)	6.71 185 (13.00)	CAS(15,14)	3.39 366 (0.04)	4.15 299 (0.03)	4.37 284 (3.56)
MRPT2(14,12)	3.96 313	4.86 255	5.76 215	ORMAS(17,14)	3.44 361 (0.02)	3.96 313 (0.08)	4.27 290 (4.91)
TD-B3LYP	4.04 307	4.72 263	5.37 231				